

# Near-field thermal radiation transfer by mesoporous metamaterials

Azadeh Didari and M. Pinar Mengüç\*

<sup>1</sup>Center for Energy, Environment and Economy (CEEE) and Faculty of Engineering, Özyeğin University, Istanbul 34794 Turkey

\*[pinar.menguc@ozyegin.edu.tr](mailto:pinar.menguc@ozyegin.edu.tr)

**Abstract:** In this work, we investigate the impact of nano-scale pores within structured metamaterials on spectral near-field radiative transfer. We use Finite Difference Time Domain Method (FDTD) and consider uniform and corrugated SiC substrates filled with rectangular nano-scale vacuum inclusions having equivalent diameters of 10, 37 and 57 nm. We report the appearance of the secondary and tertiary resonance peaks at different frequencies as a function of changing pore diameter, which cannot be predicted if an effective medium theory approximation is used.

© 2015 Optical Society of America

**OCIS codes:** (000.4430) Numerical approximation and analysis; (310.6628) Subwavelength structures, nanostructures; (010.5620) Radiative transfer; (260.2065) Effective medium theory; (300.2140) Emission; (240.5420) Polaritons.

---

## References and links

1. M. Planck, *The Theory of Heat Radiation* (P. Blakiston's Son & Co., 1914).
2. S. M. Rytov, *Theory of Electric Fluctuations and Thermal radiation* (Air Force Cambridge Research Center, 1953).
3. D. Polder and M. Van Hove, "Theory of radiative heat transfer between closely spaced bodies," *Phys. Rev.* **4**(10), 3303–3314 (1971).
4. J. J. Loomis, H. J. Maris, J. J. Loomis, and H. J. Maris, "Theory of heat transfer by evanescent electromagnetic waves," *Phys. Rev. B* **50**(24), 18517–18524 (1994).
5. J.-P. Mulet, K. Joulain, R. Carminati, and J.-J. Greffet, "Enhanced radiative heat transfer at nanometric distances," *Microscale Thermophys. Eng.* **6**(3), 209–222 (2002).
6. A. Narayanaswamy and G. Chen, "Thermal near-field radiative transfer between two spheres," *Phys. Rev. B* **77**(7), 075125 (2008).
7. C. Otey and S. Fan, "Numerically exact calculations of electromagnetic heat transfer between a dielectric sphere and a plate," *Phys. Rev. B* **84**(24), 245431 (2011).
8. M. Francoeur, M. P. Mengüç, and R. Vaillon, "Solution of near-field thermal radiation in one-dimensional layered media using dyadic Green's functions and the scattering matrix method," *J. Quantum Spectrosc. Ra.* **110**(18), 2002–2018 (2009).
9. P. Ben-Abdallah, S. A. Biehs, and K. Joulain, "Many-body radiative heat transfer theory," *Phys. Rev. Lett.* **107**(11), 114301 (2011).
10. C. J. Fu and Z. M. Zhang, "Thermal radiative properties of metamaterials and other nanostructured materials: A review," *Front. Energy Power Eng. China* **3**(1), 11–26 (2009).
11. B. J. Lee, C. J. Fu, and Z. M. Zhang, "Coherent thermal emission from one-dimensional photonic crystals," *Appl. Phys. Lett.* **87**(7), 071904 (2005).
12. C. J. Fu and Z. M. Zhang, "Further investigation of coherent thermal emission from single negative materials," *Nanoscale Microsc. Therm.* **12**(1), 83–97 (2008).
13. Z. M. Zhang, C. J. Fu, and Q. Z. Zhu, "Optical and thermal radiative properties of semiconductors related to micro/nanotechnology," *Adv. Heat Transf.* **37**, 179–296 (2003).
14. A. Kittel, W. Müller-Hirsch, J. Parisi, S. A. Biehs, D. Reddig, and M. Holthaus, "Near-field heat transfer in a scanning thermal microscope," *Phys. Rev. Lett.* **95**(22), 224301 (2005).
15. E. Rousseau, A. Siria, G. Jourdan, S. Volz, F. Comin, J. Chevrier, and J. J. Greffet, "Radiative heat transfer at the nanoscale," *Nat. Photonics* **3**(9), 514–517 (2009).
16. S. Shen, A. Narayanaswamy, and G. Chen, "Surface phonon polaritons mediated energy transfer between nanoscale gaps," *Nano Lett.* **9**(8), 2909–2913 (2009).
17. L. Hu, A. Narayanaswamy, X. Y. Chen, and G. Chen, "Near-field thermal radiation between two closely spaced glass plates exceeding Planck's blackbody radiation law," *Appl. Phys. Lett.* **92**(13), 133106 (2008).

18. A. W. Rodriguez, O. Ilic, P. Bermel, I. Celanovic, J. D. Joannopoulos, M. Soljačić, and S. G. Johnson, "Frequency-selective near-field radiative heat transfer between photonic crystal slabs: a computational approach for arbitrary geometries and materials," *Phys. Rev. Lett.* **107**(11), 114302 (2011).
19. A. Datas, D. Hirashima, and K. Hanamura, "FDTD simulation of near-field radiative heat transfer between thin films supporting surface phonon polaritons: Lessons learned," *Int. J. Therm. Sci.* **8**, 91–105 (2013).
20. A. Didari and M. P. Mengüç, "Analysis of near-field radiation transfer within nano-gaps using FDTD method," *J. Quantum Spectrosc. Ra.* **146**, 214–226 (2014).
21. A. W. Rodriguez, M. T. H. Reid, and S. G. Johnson, "Fluctuating surface-current formulation of radiative heat transfer for arbitrary geometries," *Phys. Rev. B* **86**(22), 220302 (2012).
22. S. Edalatpour and M. Francoeur, "The Thermal Discrete Dipole Approximation (T-DDA) for near-field radiative heat transfer simulations in three-dimensional arbitrary geometries," *J. Quantum Spectrosc. Ra.* **133**, 364–373 (2014).
23. M. Francoeur, M. P. Mengüç, and R. Vaillon, "Local density of electromagnetic states within a nanometric gap formed between thin films supporting surface phonon polaritons," *J. Appl. Phys.* **107**(3), 034313 (2010).
24. A. Didari and M. P. Mengüç, "Near-field thermal emission between corrugated surfaces separated by nano-gaps," *J. Quantum Spectrosc. Ra.* **158**, 43–51 (2015).
25. A. Didari and M. P. Mengüç, "Near- to far-field coherent thermal emission by surfaces coated by nanoparticles and the evaluation of effective medium theory," *Opt. Express* **23**(11), A547–A552 (2015).
26. S. A. Biehs, P. Ben-Abdallah, F. S. S. Rosa, K. Joulain, and J. J. Greffet, "Nanoscale heat flux between nanoporous materials," *Opt. Express* **19**(S5), A1088–A1103 (2011).
27. J. Li, Y. Feng, X. Zhang, C. Huang, and G. Wang, "Near-field radiative heat transfer across a pore and its effects on thermal conductivity of mesoporous silica," *Phys. B-Condensed Matter* **456**, 237–243 (2015).
28. P. Liu and G. F. Chen, *Porous Materials: Processing and Applications* (Elsevier, 2014).

---

## 1. Introduction

Max Planck's law of blackbody radiation helped profoundly with the establishment of the theory of thermal radiation in the early 20th century. Although Planck's treatise, *Theory of Heat Radiation* [1], was extremely versatile and applicable to large number of physical cases, it fails to explain the rich physics at length-scales much smaller than the wavelength of radiation. In 1950s, the general framework of fluctuational electrodynamics was proposed by Rytov [2]. In 1971, Polder and Van Hove presented their well-recognized theory of radiative heat transfer between closely spaced bodies [3]. In the years that followed, the study of near-field thermal radiation transfer in geometries containing nano-scale gap sizes in which the geometric size is comparable to the characteristic wavelength of thermal radiation  $\lambda_{th} = hc / k_B T$  as defined by the Wien law, has gained significant attention. Analytical studies of structures such as two bulks [3–5], sphere-sphere [6], sphere-plate [7] 1D layered media [8] and nanoparticles modeled as electric point dipoles [9] have been reported in the literature. Furthermore, nanotechnology-based techniques have been investigated widely in the past decade with the intention to alter the development of metamaterials [10]. Coherent thermal emission is investigated [11,12] and radiative properties of photonic crystals and porous silicon is reported [13]. Experimental investigations confirming the theoretical predictions have also been outlined, including tip-plate [14], sphere-plate [15,16] and plate-plate configurations [17]. When considering complex systems, containing irregular shapes, an exact solution may not be easily found due to existing asperities in the geometries and the mathematical difficulties involved. In such scenarios, numerical techniques could be used to obtain a solution [18–22]. Depending on the specifications of the problem in hand, such numerical methods may involve discretization of a given surface or the entire volume of the geometry and by obtaining the electromagnetic field characteristics in each cell and then integration over the surface or volume in order to obtain the desired results.

In our recent paper [20], we have presented a series of results for the near-field radiative transfer (NFRT) based on Finite Difference Time Domain (FDTD) method for flat, uniform, thin SiC films supporting surface phonon polaritons separated by a vacuum nano-gaps forming a sandwich-structure. These results showed a good agreement with the analytical results presented in [23], giving confidence in the robustness of the model and the algorithm. We then extended the solution to corrugated surfaces and studied the effects of shape, size and

periodicity of nanostructures on the near-field thermal emission [24]. The comparison of FDTD and the Effective Medium Theory (EMT) results for near-to far field thermal emission and radiation studies was given in [25] where it was concluded that EMT may not be accurate when the edge effects in complex geometries have to be considered.

In the present work, we explore the near-field radiative heat transfer in porous metamaterials of thin films, which are considered to be either uniform or having nanostructures on them; they may also contain uniformly distributed nano-size pores within (see Fig. 1). For simulations, the emitting and non-emitting layers are assumed to be 100 nm and 10 nm thick SiC films with the separating vacuum gap of 100 nm. The width and the height of nanoparticles (NPs) on emitting layer are designated as ‘ $w$ ’ and ‘ $h$ ’ respectively, as shown in Fig. 1. In the simulations, the values of  $w = 500 \text{ nm}$  and  $h = 20 \text{ nm}$  are used and the horizontal distance ‘ $d_n$ ’ between them is kept at 50 nm. We designate the equivalent diameter of the pores as  $D_{eq}$ , and they are considered as rectangles in the simulations, where the width  $P_w = 50 \text{ nm}$  and the height  $P_h = 30 \text{ nm}$  are chosen. Here, the equivalent diameter is defined as  $D_{eq} = 2 \times (P_w \times P_h) / (P_w + P_h)$ . The horizontal spacing between the pores is set to 50 nm and the vertical spacing is 2 nm. The emitting layer is assumed to have temperature of  $T = 1000 \text{ K}$  and the non-emitting layer is kept at  $T = 0 \text{ K}$ .

First, we present the results for the Local Density of Electromagnetic States (LDOS) for different configurations. We then report the near-field emission and near-field heat flux profiles for different scenarios. Then, we identify the profiles in which maximum rate of radiative heat transfer is obtained. The comparisons between FDTD and EMT analysis are made afterwards which accentuates the possible weaknesses of EMT in providing accurate results when dealing with porous metamaterials. After obtaining the results for the benchmark scenario in which both layers are non-porous SiC thin layers separated by the vacuum gap, we provide a comparison between the benchmark scenario against the scenario in which the emitting layer is a porous SiC filled with vacuum inclusions with equivalent diameters  $D_{eq}$  of 10, 37 and 57 nm, respectively. Particular emphasis is to be given to the appearance of the additional resonance peaks obtained when there are nano-pores within the emitting layer.

## 2. Methodology

In order to present the implementation of FDTD, we write the Maxwell equations in terms of the electrical displacement and magnetic fields  $D_x$ ,  $D_z$  and  $H_y$  respectively. They are considered for Transverse Magnetic (TM) wave, in which the only non-zero component of magnetic field is  $H_y$ , i.e. propagation along the  $z$  axis. FDTD analysis is performed for scenarios in which the emitting film is inhomogeneous, anisotropic, nonmagnetic, and the non-emitting film is homogenous and isotropic. Both films are described by a frequency-dependent dielectric function given by Drude-Lorentz’s permittivity model. We do not provide the FDTD formulations here, as the details are available in [20,24]. The two important studies which discuss the effects of pores on the near-field radiation transfer are those by Biehs et al. [26] and Li et al. [27]. In [26], Biehs et al. reported the heat flux between nanoporous materials through an EMT calculation where both layers were air filled porous SiC [26]. In [27] Li et al. showed experimentally that when mesoporous Silica material was used for pore sizes between 2 and 50 nm, the near-field heat flux was enhanced by orders of magnitude when compared with non-porous Silica. Here, we thoroughly investigate the behaviour of near-field thermal emission/radiation of a porous SiC emitting layer having pores with the equivalent diameters of 10, 37 and 57 nm, respectively. The main reason for the choice of these pore sizes came from Li et al. [27] where they discussed that when the diameter of the pore is much smaller than the thermal wavelength, the electromagnetic field across the pore is dominated by the near-field radiation, and the combined thermal conductivities of mesoporous Silica decreases gradually with the pore diameter increasing.

They report that when the pore's diameter is smaller than 50 nm (mesoporous pores) the enhancement rate is higher than when compared against the porous materials having pore diameters larger than 50 nm. For this reason, we chose the size of the pores (width and height) such that the equivalent diameter would become smaller and larger than 50 nm. Furthermore, the results are also compared against those obtained from the equivalent EMT analysis. In order to implement the EMT, the total surface area of the vacuum voids is calculated (in 3D it would be total volume) and is then subtracted from the surface area of the porous SiC material. The result corresponds to an isotropic SiC layer of a reduced thickness and the LDOS is recalculated using the same vacuum gap size and non-emitting SiC layer. The results and our observations are discussed in the next section.

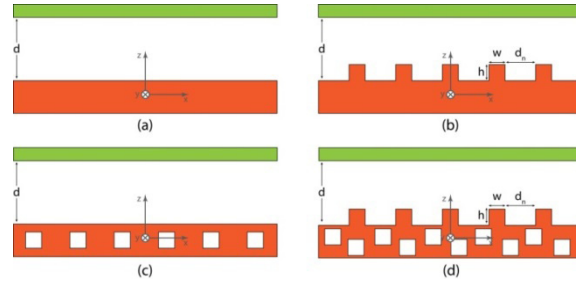


Fig. 1. a) Perfectly-flat parallel thin films separated by nano-gap (emitting layer at the bottom, non-emitting layer on top). b) Rectangular nanoparticles placed on the emitting film separated by nano-gap from non-emitting film. c) Porous SiC emitting layer separated by a vacuum gap from non-porous SiC non-emitting layer. d) Corrugated porous SiC emitting layer separated by a vacuum gap from non-porous SiC non-emitting layer.

### 3. Results and discussions

We first investigate the impact of nano-pore sizes of 10, 37 and 57 nm within SiC structure on the LDOS profiles and present the results in Figs. 2, 3 and 4, respectively. These results are found at 30 nm above the emitting layer, and are normalized to the peak of the benchmark scenario. Our observations show that when  $D_{eq}$  is either 10 or 37 nm, the near-field thermal emission shows a significantly larger magnitude than the benchmark case or when compared against the case where the non-porous emitting layer is corrugated. Figure 2 depicts the results of comparison between benchmark case against the scenarios in which LDOS results for porous emitting layer is obtained through the FDTD and the EMT simulations. These results are then compared against the case for porous medium. Introducing porosity in SiC emitting layer increases the magnitude of LDOS and produces an additional resonant peak when the pore sizes are small which shows the potential of this structures to produce additional spectral characteristics. The physical mechanism for the appearance of the additional resonance peaks may be associated with the strong coupling of the pores' cavity resonances with those stemming from the surface phonon polaritons. The additional enhancement introduced by the porous emitting layer could be associated with the fact that the dominance of the p-polarized contribution in the near-field regime becomes even greater when having vacuum inclusions. Our studies show that when the horizontal distance between the pores is increased, the magnitude of the peaks decreases and eventually the additional peak vanishes when the pores' horizontal spacing reaches to 150 nm. It is apparent that beyond a given distance, the coupling does not take place. On the other hand, if we replace the emitting smooth layer with a corrugated porous layer, we observe that the enhancement rates are higher. The equivalent EMT analysis for these case studies can neither produce the same enhancement rates nor could show the additional resonant peaks. In Fig. 2 (left), we compare the results when  $D_{eq} = 10$  nm, for porous SiC emitting layer against the benchmark scenario, where the SiC resonant

peak occurs at  $1.79 \times 10^{14}$  rad/s. It is important to note that we have 73% spectral enhancement in the LDOS profile here. Similarly, as seen in Fig. 2 (right), for  $D_{eq} = 37$  nm, the enhancement is 73%, and for the case of  $D_{eq} = 57$  nm, in Fig. 3, the enhancement is about 66%. The appearance of the second resonant peak at  $1.63 \times 10^{14}$  rad/s is clear for the case of  $D_{eq} = 37$  nm. This pattern is also observed for  $D_{eq} = 10$  nm; however, in this case two additional peaks are apparent at  $1.61 \times 10^{14}$  rad/s and  $1.66 \times 10^{14}$  rad/s, respectively. It is also noted that when  $D_{eq}$  of pores is smaller than 37 nm (for instance,  $D_{eq} = 20$  nm (not shown) and for  $D_{eq} = 10$  nm), the resonance frequency shifts towards smaller frequencies in porous SiC and the resonance peak occurs at  $1.77 \times 10^{14}$  rad/s. When  $D_{eq} = 57$  nm, no additional resonant peak or shift in resonance frequency are observed. The enhancement due to near-field radiative transfer decreases as the pore diameter increases from 10 nm to 37 nm and then to 57 nm. Another important factor to consider in a porous medium is the impact of the porosity, defined as the ratio of the pore volume to the entire nominal volume of a porous body [28]. Porosity percent for 10, 37, 57 nm effective sizes was found to be 16%, 46% and 40%, respectively.

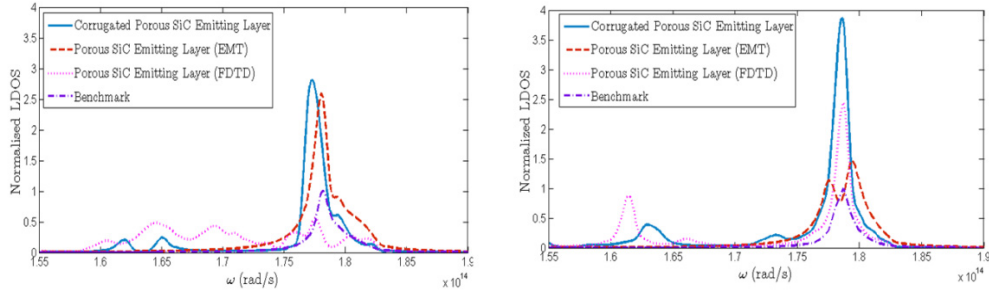


Fig. 2. Comparison of LDOS profile for benchmark scenario found through FDTD and EMT analysis for porous SiC emitting layer against corrugated porous emitting layer having  $D_{eq} = 10$  nm (left) and  $D_{eq} = 37$  nm (right).

These results clearly reveal the significant deviation between the FDTD and the EMT simulations. It might be concluded that this discrepancy is due to the fact that the conventional EMT is incapable of describing systems where the change in dielectric permittivity from layer to layer is large. This usually happens when the medium is comprised of a metamaterial adjacent to any other medium with a much different permittivity such as vacuum.

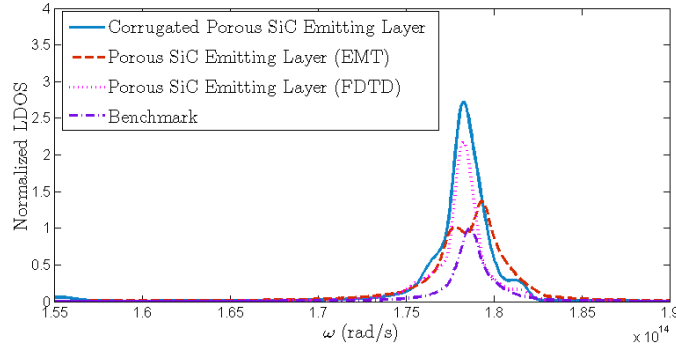


Fig. 3. Comparisons of the normalized LDOS profiles for the benchmark case and that for the corrugated porous emitting SiC layer with  $D_{eq} = 57$  nm as obtained from the FDTD and the EMT simulations.

Figure 4 (left) shows the near-field heat flux profiles at  $T = 1000$  K for the benchmark case compared against that where the emitting layer is a corrugated porous SiC with  $D_{eq} = 37$  nm. The results are normalized to the peak of the benchmark scenario. We observed that about 75% spectral enhancement can be achieved for near-field heat flux profiles through such configurations. Figure 4 (right) shows the coupling effect of pores which changes the nature of the spectral near-field radiative transfer. As the separation between the nano-pores is changed from 50 nm to 150 nm the second peak diminishes, and at 200 nm separation it becomes invisible. This suggests that the appearance of the secondary and tertiary peaks is due to the coupling of pores' internal cavity resonances with those of surface phonon polaritons due to the nano-gaps between SiC films. Further study of this interaction is needed and being conducted.

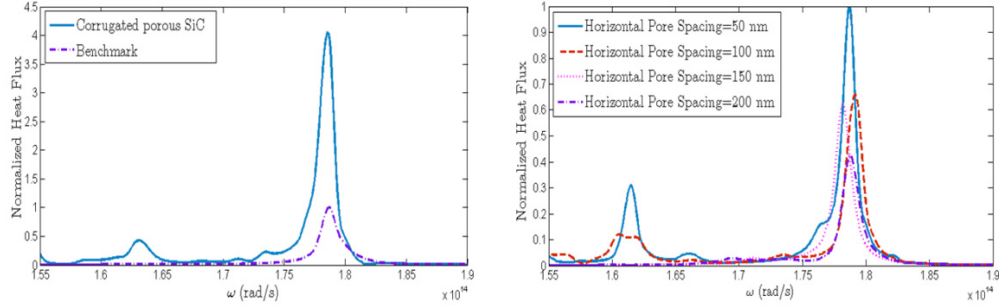


Fig. 4. (Left) Comparison of normalized heat flux profiles for the benchmark case against a corrugated porous SiC emitting layer of  $D_{eq} = 37$  nm. (Right) Impact of horizontal pore spacing on normalized heat flux profile,  $D_{eq} = 37$  nm.

#### 4. Conclusions

In this paper, we investigated the behaviors of the LDOS, near-field heat flux and the radiative emission profiles for corrugated, porous as well as both corrugated and porous SiC emitting layers. In our configurations, we considered corrugations by NPs of  $w = 500$  nm and  $h = 20$  nm and  $D_n = 50$  nm, and pore width  $P_w = 50$  nm and pore height  $P_h = 30$  nm were kept the same everywhere throughout this work. We considered the presence of rectangular corrugations on the surface of thin film and rectangular vacuum inclusions of equivalent diameters of 10, 37 and 57 nm. We report for the first time the presence of additional resonance frequency peaks for corrugated porous SiC emitting layers. The results suggest that mesoporous SiC emitting layer can increase the near-field LDOS and the near-field heat transfer by orders of magnitudes. Corrugated mesoporous SiC emitting layer has shown even more enhancement when compared against the non-porous SiC used in the same configuration. In addition, they depict an additional resonance peak which can be tuned as a function of pore size and material use. Such mesoporous structures can enhance near-field thermal radiation, which allows the researchers to construct designer mesoporous metamaterials for specific applications for sensing, energy harvesting, selective nano-scale manufacturing, radiative cooling, heat-assisted magnetic recording, among others.

#### Acknowledgments

This project was partially funded by TUBITAK-1001 (Grant No.109M170) and FP-7-PEOPLE-IRG-2008 (Grant No.239382 NF-RAD) at Özyegin University, Istanbul, Turkey. AD is funded by CEEE at Özyegin University.